Prediction of casting mechanical parameters based on direct microstructure image analysis using deep neural network and graphite forms classification

Bartlomiej Sniezynski[1[0000−0002−4206−9052]],
Dorota Wilk-Kolodziejczyk[1,2[0000−0001−5590−0477]], Radosław Łazarz[1[0000−0002−3151−9759]], and
Krzysztof Jaskowiec[1,2]

[1] AGH University of Science and Technology, Krakow, Poland
bartlomiej.sniezynski@agh.edu.pl, dwilk@agh.edu.pl, lazarz@agh.edu.pl
[2] Łukasiewicz Research Network – Kraków Institute of Technology

Abstract. This paper presents methods of prediction of casting mechanical parameters based on direct microstructure image analysis using deep neural networks and graphite forms recognition and classification. These methods are applied to predict tensile strength of iron-carbon alloys based on microstructure photos taken with the light-optical microscopy technique, but are general and can be adapted to other applications. In the first approach EfficientNet architecture is used. In the second approach graphite structures are separated, recognized using VGG19 network, counted and classified using support vector machines, decision trees, random forest, logistic regression, multi-layer perceptron and AdaBoost. Accuracy of the first approach is better. However, the second allows to create a classifier, for which the accuracy is also high, and can be easily analyzed by human expert.

Keywords: Prediction of mechanical properties · Microstructure image analysis · Deep neural network · Graphite forms classification.

1 Introduction

The main goal of this work is to present two methods for prediction of the mechanical parameters of castings based on the analysis of the microstructure image.

Initially, the prediction of mechanical properties was based on the analysis of phase diagrams. However, already in the 80s it was indicated that these techniques will be replaced by mathematical models and artificial intelligence methods [18]. In early works, neural networks were applied to predict Ferrite Number (FN) based on weight percentage of 13 elements [15, 28]. In our research we also started with machine learning methods applied to process parameters

ICCS Camera Ready Version 2023
To cite this paper please use the final published version:
DOI: 10.1007/978-3-031-36030-5_42

and chemical composition [29]. However, approach described this paper is based on microstructure image classification.

In [3] Deep Neural Networks are applied for lath-bainite segmentation in complex-phase steel. Vanilla U-Net and VGG16 neural architectures are used. In our research, which is continuation of work [11], we predict tensile strength of iron-carbon alloys based on microstructure photos taken with the Light-Optical Microscopy (LOM) technique. The first approach is similar to one proposed in [3] – EfficientNet deep neural network is applied to process the images directly. In the second approach, which is our main contribution, graphite structures are extracted from the image, and their types (forms) are recognized using VGG19 network. Feature vector consists of numbers of graphite structures assigned to every type. Classification algorithm is used to predict tensile strength based on these features. We have applied support vector machines, decision trees, random forest, logistic regression, multi-layer perceptron and AdaBoost. Performance measured by F1 score of the first approach was better in evaluation. However, the second approach allows to create classifier which can be easily analyzed by human expert. This method garnered a lot of positive feedback from domain experts because it was not a black box solution.

Another important contribution of this research is creation of a dataset consisting of microstructure images of ductile iron and their labels from a number of experiments that was used in evaluation. This dataset will be made available to interested researchers upon email request.

In the following sections related research and methodology are presented. Next experiments are described. Conclusions and future works summarize the paper.

2 Related Research

Metal-characterising properties have been a consistent subject of scientific interest for many years, due to their significant industrial importance. Consequently, various historical works attempted to automatically predict their actual values [15, 21, 5]. One of the first worth noting was the research conducted by Babu et al. [5], who proposed a model for predicting ferrite numbers exhibiting accuracy comparable to that of WRC-1992. Notably, this model was later improved even further by Vitek et al [28].

Classical machine learning techniques yielded similarly promising results for other analogous tasks. For instance, Badmos et al. [6] investigated prediction quality for a large array of traits, such as tensile strength, durability, hardness, and deformation rate. Similarly, Javier et al. [12] examined chemical composition, casting size, cooling speed, and thermal treatment using linear classification, k-nearest neighbours, decision trees, and Bayesian networks (BN). Yuxuan et al. [30] used a simple neural network with 20 input variables (such as chemical composition, heat treatment conditions, and test temperature) to predict the tensile characteristics of stainless steel. Additionally, as showcased by Penya et.

ICCS Camera Ready Version 2023
To cite this paper please use the final published version:
DOI: 10.1007/978-3-031-36030-5_42

al. [20], BNs were successfully applied to recognise the presence of micro-damages in the casting exhibited before or during the casting process itself.

Sachin et al. [22] incorporated data from electron backscatter diffraction (EBSD) and designed a way to effectively identify and quantify ferrite micronutrients in complex microstructures of various steel grades. However, in a report authored by Britz et al. [9], a correlation approach based on EBSD and LOM was used — instead of using those common methods independently. Finally, a work by Gola et al. [13] dealt with the classification of the components of the microstructure of low-carbon steel by employing a data mining approach.

Presently, the employment of deep neural networks has become the prevalent approach for image-driven prediction tasks, with convolutional architectures [27] or transformers [8] being particularly favoured. Research by Durmaz et al. [3] applied U-Net networks for structure segmentation in complex phase steel, and similar methods have been effective in predicting the properties of castings [4]. In this research, transfer learning through the VGG19 [24] architecture was utilized for microstructure-based classification, while the simpler direct classification was carried out using EfficientNet [25].

3 Methodology

3.1 Direct image classification using deep neural networks

The primary aim of this approach is to establish a baseline for the casting quality prediction task (a binary classification problem, where one has to distinguish low tensile strength samples from those characterised by high R_m values) without over-engineering the pipeline for this specific problem. To achieve this objective, we treated the target classifier as a single-step black box and ignored the domain-specific knowledge used by the other presented approaches. Due to the limited size of the utilised dataset, we determined that employing a dedicated architecture would offer minimal advantages and may even lead to indirect overfitting. Similarly, interpretability concerns are postponed to the future works, as they were not the critical focus. Thus, we concentrated on well-established pre-trained techniques with a proven record of successful deployments.

Our initial search for a suitable foundational model showed that vanilla VGG-like arrangement [24] is enough for single graphite structure classification (see below) but together with the deep residual network ResNet50 [10] is severely underperforming in direct microstructure image classification when compared with the third candidate — a group of convolutional networks jointly known as the EfficientNets [25].

EfficientNets represent a family of convolutional networks specifically designed to balance model depth, width, and resolution. They leverage a scalable architecture that can be tuned to various sizes while maintaining a consistent level of accuracy. The main building block of EfficientNets is the mobile inverted bottleneck, first introduced as a part of the MobileNetV2 network [23]. More recently, the machine vision community proposed numerous other architectures as

ICCS Camera Ready Version 2023
To cite this paper please use the final published version:
DOI: 10.1007/978-3-031-36030-5_42

their successors, including EfficientNetV2 [26] (with its potentially faster fused residual blocks) and ConvNeXt [16] (proven to be a viable alternative even to the modern vision transformer models). However, we remain convinced that the original EfficientNets are still the safest choice for establishing a realistic and reproducible baseline result, mainly due to the sheer number of successful applicative studies profiting from them.

We employed the largest member of the family - the B7 model consisting of 66 million weights, pre-trained on the ImageNet dataset. The task of cast iron assessment significantly deviates from the standard object recognition problems. Specifically, the input images are near-monochromatic and uniformly filled with content. Consequently, fine-tuning the entire network (instead of adjusting only the top fully-connected layers) was deemed advantageous.

To pick the hyperparameters for the fine-tuning process, we utilised the AutoKeras meta-optimisation system [14]. The complete configuration consisted of the elements listed in Table 1. The automatic tuner itself is a hybrid oracle that performs a chosen number of trials (50 in our case). First, it aggregates parameters into conceptual categories (e.g. "augmentation" or "architecture"). Then, it generates new values for one category at a time with a greedy strategy — while using the best result obtained so far for the rest.

Table 1. EfficientNet fine-tuning parameters

Hyperparameter	The set of considered values
Adam learning rate (α)	$\{0.001, 0.0001, 0.00002\}$
top layers spatial reduction (t_s)	$\{\textsc{GlobalAverage}, \textsc{GlobalMax}\}$
classification head dropout rate (p_d)	$\{0.0, 0.25, 0.5\}$
translation augmentation factor (g_t)	$\{0.0, 0.2\}$
zoom augmentation factor (g_z)	$\{0.0, 0.2\}$
contrast augmentation factor (g_c)	$\{0.0, 0.2\}$
rotation augmentation factor (g_r)	$\{0.0, 0.2, 0.5\}$
horizontal flip (g_h)	$\{0, 1\}$
vertical flip (g_v)	$\{0, 1\}$

Both the parameter selection and the actual fine-tuning operated on a collection of images that were initially of varying sizes and aspect ratios. To ensure consistency, we first applied a pre-processing step in which each image was cropped to a square shape and rescaled to a resolution of 224x224 — resulting in 3525 positive (high R_m) and 1455 negative (low R_m) samples.

The reported scores were obtained as a result of a standard 10-fold cross-validation procedure. In the case of the first analysed fold, the training set was additionally subdivided into two smaller subsets (in a ratio of 8 to 2). Those subsets were utilised to conduct an initial AutoKeras hyperparameter search. The winning arrangement of parameters obtained that way was then saved and used unchanged throughout all the remaining folds of the experiment.

ICCS Camera Ready Version 2023
To cite this paper please use the final published version:
DOI: 10.1007/978-3-031-36030-5_42

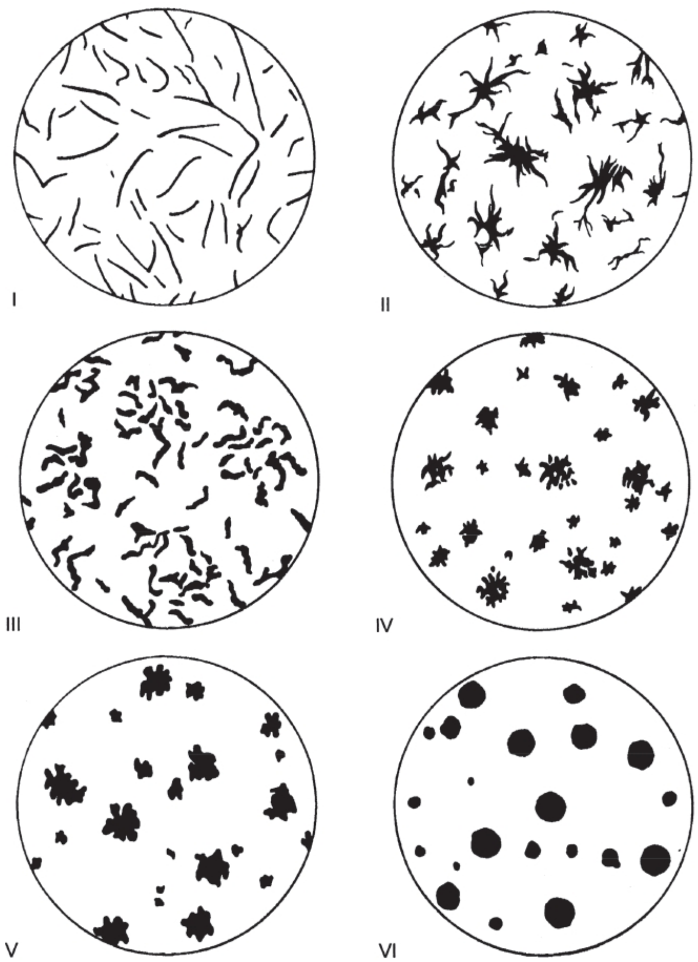

Fig. 1. Graphit forms in cast irons [1]

3.2 Microstructure-based classification

Microstructure-based classification idea is based on analysing graphite structures appearing in the microstrucutre LOM picture. According to the norms [1], the structures can be classified into six principal forms, which are presented in Figure 1.

The algorithm gets LOM picture and mechanical property prediction model as input and returns predicted property, see Algorithm 1. At the beginning graphite structure type counters are initialized with 0 (lines 1-3), next separate graphite structures are distinguished in the picture P (line 4) and stored in a list S. These structures are classified to one of the structure types t and a number of structures for recognized type is updated (lines 5-8). These numbers form

ICCS Camera Ready Version 2023
To cite this paper please use the final published version:
DOI: 10.1007/978-3-031-36030-5_42

a feature vector X describing the picture. Next, mechanical property can be predicted using model M (line 9).

Input: P – LOM picture, M – mechanical property prediction model
Output: Predicted mechanical property
1 **foreach** *structure type* t **do**
2 | $X[t] \leftarrow 0$
3 **end**
4 $S \leftarrow$ Separate structures in picture P;
5 **foreach** *structure picture* $s \in S$ **do**
6 | $t \leftarrow$ type of structure s;
7 | $X[t] \leftarrow X[t] + 1$;
8 **end**
9 $c \leftarrow$ prediction of mechanical property $M(X)$;
10 **return** c;

Algorithm 1: Microstructure-based classification

This algorithm depends on three main procedures that should be specified: structure separation (line 4), structure type classification (line 6) and mechanical properties prediction (line 9). They are described below.

Structure separation To separate the structures, their edges are discovered using Canny's edge detection [7] approach. For every separate edge region, part of the image surrounded by the edge is cut off and put in the middle of a white rectangle (dimensions 335 x 251 pixels were used in experiments). It happens that several graphite structures are in contact with each other and recognized as one, big structure. Frequency of such error is very low, below 1%.

Structure type classification To determine type of the separated structures, VGG19 convolutional neural network [24] and transfer learning were applied. The last three layers of VGG19 were replaced by three fully connected layers consisting of 512 neurons each and softmax output layer. These last layers were updated during training on examples of forms of graphite structures that were manually assigned to one of six forms (Fig. 1), to which additional type 0 form, containing merged structures described above, was created.

To improve quality of classification three transformations were tried. Data augmentation was used to balance the data. Gaussian blur was applied to merge cracked structures. Image thresholding was also applied to decrease color depth to 1-bit and eliminate gray levels.

Mechanical properties prediction In our research several machine learning algorithms were applied to build the model M predicting mechanical properties of casting represented by the feature vector X. Mechanical property was categorical and represented low and high tensile strength. However, presented approach is general and can be also used for other properties.

ICCS Camera Ready Version 2023
To cite this paper please use the final published version:
DOI: 10.1007/978-3-031-36030-5_42

The following algorithms were applied for classification: Support vector machines, decision trees (CART algorithm), random forest, logistic regression, multi-layer perceptron and AdaBoost. Training data were only lightly unbalanced (3358 examples with high tensile strength versus 1337 with low). Training was also applied for balanced data (using random elimination of examples from over-represented category), but results were worse than on the original training data. Data augmentation techniques could be applied here but this topic is left for future research.

4 Experiments

4.1 Source data

Photos of microstructures subjected to classification were created as a result of experiments (research projects) carried out in the former Foundry Research Institute in Krakow (currently Łukasiewicz Research Network - Krakow Institute of Technology). The basis for the classification was the information contained in the standards regarding the shape of graphite and qualifying them to the appropriate groups / classes. Another issue that should be taken into account when classifying the microstructure is the possibility of defects related to the arrangement of the graphite precipitate. The size of the precipitates and significant differences in the size of the precipitates may be an important factor. The best mechanical properties can be obtained with spheroidal graphite compared to cast iron with flake precipitates. When observing the microstructure of cast iron with flake graphite, defects related to graphite degeneration may also occur, which also deteriorate the mechanical properties.

The set consists of 223 images in two magnification levels: a hundredfold and five hundredfold magnification. Images with lower magnification have resolution 2080x1540 and with higher 1388x1040. Samples were manually classified by domain expert according to tensile strength R_m. Examples of these images are presented in Fig. 2. All images are in RGB format. Images with a hundredfold magnification are cut into 25 smaller pictures to achieve five hundredfold magnification.

Based on CRISP-DM methodology pictures with low quality and large amount of noise were removed, together with pictures done other than LOM technique and representing other types of castings, see Fig. 2-(c) for example.

4.2 Direct classification

The initial hyperparameter search concluded by finding the following arrangement: $\alpha = 0.00002$, $t_s = \textsc{GlobalAverage}$, $p_d = 0.0$, $g_t = 0.2$, $g_z = 0.0$, $g_c = 0.0$, $g_r = 0.5$, $g_h = 1$, $g_v = 1$. The gathered values are in line with our prior knowledge and expectations about the problem domain. The images of cast iron microstructures do not have a natural orientation, i.e., they have no inherent concept of top, bottom, left, right, or centre. This means that they can be freely

ICCS Camera Ready Version 2023
To cite this paper please use the final published version:
DOI: 10.1007/978-3-031-36030-5_42

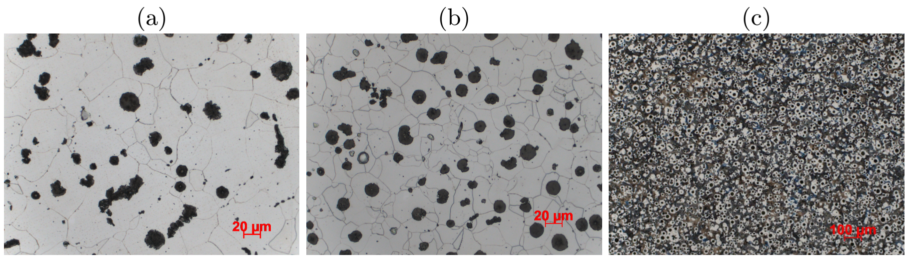

Fig. 2. Examples of LOM images representing microstructure of iron-carbon alloys with low tensile strength (a), high tensile strength (b) and outlier image removed from the training data set (c)

flipped, rotated, and shifted without affecting the representation of the underlying structures. Hence, we can easily augment our training dataset by applying those transformations to the images, without risking a negative impact on the accuracy of the final model.

The preference for low learning rates supports our decision to start with a pre-trained model, implying that a slight correction of the initial weights was enough to achieve satisfactory results for the studied problem. Finally, we acknowledge that the observed leaning towards less regularization may be a byproduct of the assumed limited epoch budget, where training was halted after 30 epochs. This is due to the fact that high-dropout networks tend to converge more slowly than their no-dropout counterparts.

Table 2 outlines the aggregated experiment results obtained for the aforementioned optimal parameter set. The small number of the utilised samples resulted in a significant between-fold variance and score deviation. The same phenomenon can be spotted when scrutinising Figure 3: there are two clear outliers among the ROC trends, corresponding to splits that are harder to classify. On the other hand, the healthy shape of the discussed curves and the good balance between the calculated precision and recall metrics show that, fortunately, the skewed class distribution in the training set had a negligible effect on the ultimately attained performance.

4.3 Microstructure-based classification

Structure type classification Training data for structure form classification consisted of 1572 examples. Numbers of examples in every category are presented in Table 3. The network was trained in 100 epochs using Adam optimizer. Accuracy of the trained network was equal to 82% on test data (10% of the training data).

Table 2. Baseline results of a direct classification with a fine-tuned EfficientNet

Accuracy	Precision	Recall	F1 Score	AUC
$90.9\% \pm 1.4\%$	$92.9\% \pm 1.7\%$	$94.3\% \pm 2.1\%$	$93.6\% \pm 1.1\%$	$96.44\% \pm 0.93\%$

ICCS Camera Ready Version 2023
To cite this paper please use the final published version:
DOI: 10.1007/978-3-031-36030-5_42

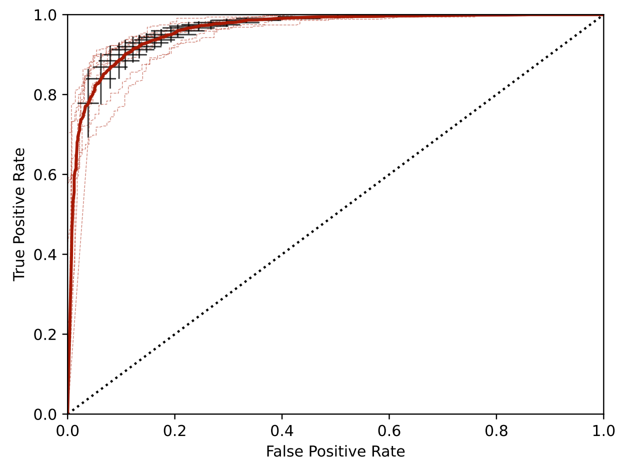

Fig. 3. Receiver Operating Characteristic (ROC) curves for direct classification. Dark red line denotes the mean ROC curve, black crosses — its standard deviation in certain points, dotted light red lines — the curves corresponding to cross-validation splits.

F1 metrics was equal to 0.79. As it may be noticed in confusion matrix generated for types I-VI, which is presented in Fig. 4, the main problem is distinguishing form IV, which is mistaken with III and V. Also form II is mistaken with form III and I.

Accuracy of structure form classification using VGG19 convolutional neural network trained on data with various transformations applied are presented in Tab. 4. Augmentation resulted in drop of accuracy. Adding Gaussian blur allowed to improve results for classes V and VI. However, other classes were miss-classified more often (especially I and II). Therefore the overall improvement was minimal. Image thresholding resulted in accuracy decrease.

Mechanical properties prediction Results obtained in 10-fold cross-validation for chosen algorithms are presented in Tab. 5. Hyper-parameters of these algorithms

Table 3. Number of examples in every form type

Form	Number of examples
0	14
I	278
II	122
III	292
IV	76
V	289
VI	501

ICCS Camera Ready Version 2023
To cite this paper please use the final published version:
DOI: 10.1007/978-3-031-36030-5_42

Fig. 4. Confusion matrix for VGG19 convolutional neural network for structure form classification

were tuned using Optuna framework [2]. Models were trained on original and balanced data. As we can see, the best Accuracy and Log loss achieved AdaBoost (83,4%, 0.67). The highest F1 values were achieved by Support vector machine and Random forest (0.90). The best Average precision achieved Random forest and AdaBoost. Accuracy of the reset of algorithms is similar. Other metrics differ more.

What can be also observed, results for balanced data are worse than for unbalanced. Better balancing techniques should be applied in the future to check their influence.

Because Decision tree algorithm achieved results close to the best models, decision trees learned were analyzed and consulted with domain expert. Example of such decision tree is presented in Fig. 5. Its accuracy is 81.2%. The expert confirmed that the decision tree is consistent with the domain knowledge.

Table 4. Accuracy of structure form classification using VGG19 convolutional neural network trained on data with various transformations applied

Augmentation	Gaussian blur	Thresholding	Accuracy
No	No	No	82.2%
Yes	No	No	78.0%
Yes	Yes	No	79.7%
Yes	Yes	Yes	77.1%

ICCS Camera Ready Version 2023
To cite this paper please use the final published version:
DOI: 10.1007/978-3-031-36030-5_42

Table 5. Results of chosen machine learning algorithms applied to mechanical properties prediction

Model	Balanced data	Accuracy	Log loss	F1	Average precision
Support vector machine	No	83.3%	0.39	**0.90**	0.90
Support vector machine	Yes	76.9%	0.49	0.78	0.81
Decision tree	No	81.6%	0.46	0.89	0.81
Decision tree	Yes	69.5%	0.58	0.74	0.65
Random forest	No	83.3%	0.40	**0.90**	**0.92**
Random forest	Yes	78.4%	0.47	0.79	0.83
Logistic regression	No	82.2%	0.41	0.89	0.91
Logistic regression	Yes	77.1%	0.52	0.78	0.80
Multilayer perceptron	No	82.7%	0.41	0.88	0.91
Multilayer perceptron	Yes	80.6%	0.46	0.83	0.84
AdaBoost	No	**83.4%**	**0.67**	0.89	**0.92**
AdaBoost	Yes	72.0%	0.62	0.76	0.77

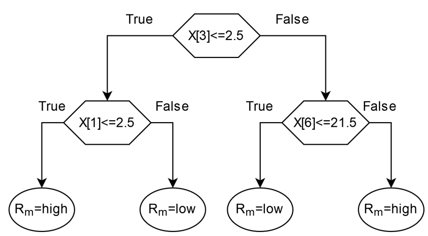

Fig. 5. Sample decision tree for mechanical properties prediction

5 Conclusions

In this paper we have shown that it is possible to predict casting mechanical parameters based on direct microstructure image analysis and recognition and classification of graphite forms. These methods were applied to predict tensile strength of iron-carbon alloys, but they can be used to predict other parameters too.

Direct image classification has better accuracy (90.1%) and F1 metrics (93.6%) than recognition and classification of graphite forms. However the latter approach allows to create models with high interpretability and still high accuracy. Decision tree allows to achieve accuracy equal to 83.3% and F1 equal to 90%, and the model learned is very simple. It was consulted with domain experts and they confirmed that it is consistent with their knowledge.

Interpretability of the model is especially important in decision support systems. Application of such a model would allow to add explanation functionality, which is very important in engineering.

In the future research we are planning to apply Grad-CAM for producing visual explanations for direct microstructure image analysis. We would like to apply other methods for data augmentation in recognition of graphite forms and

ICCS Camera Ready Version 2023
To cite this paper please use the final published version:
DOI: 10.1007/978-3-031-36030-5_42

other architectures than VGG19 for structure classification. We would also like to use other methods with symbolic knowledge representation for classification, e.g. scoring systems [19] that we have applied in medical domains or rule based systems, which correspond to human way of thinking well [17]. Last but not least, we would like to apply this methodology for prediction of other mechanical properties, like elastic limit (R_p) of iron-carbon alloys.

Acknowledgements This paper received partial support from the funds assigned by the Polish Ministry of Education and Science to AGH University. Authors would like to thank Wiktor Reczek for help with Microstructure-based classification programming and experiments.

References

1. EN ISO 945-1:2018 Microstructure of cast irons – Part 1: Graphite classification by visual analysis (ISO 945-1:2017) (2018)
2. Akiba, T., Sano, S., Yanase, T., Ohta, T., Koyama, M.: Optuna: A next-generation hyperparameter optimization framework. In: Proceedings of the 25th ACM SIGKDD international conference on knowledge discovery & data mining. pp. 2623–2631 (2019)
3. Ali, D., Martin, M., Bo, L., Akhil, T., Dominik, B., Elizabeth, H., Chris, E., Frank, M., Peter, G.: A deep learning approach for complex microstructure inference. Nature Communications **21**, 1–15 (2021)
4. Anke, S., Peter, B.: Machine learning for material characterization with an application for predicting mechanical properties. Special Issue: Scientific Machine Learning - Part I **44**(1), 1–21 (2021)
5. Babu, S.S., Vitek, J.M., Iskander, Y.S., David, S.A.: New model for prediction of ferrite number of stainless steel welds. Science and Technology of Welding and Joining pp. 279–285 (1997)
6. Badmos, A., Bhadeshia, H.: Tensile properties of mechanically alloyed oxide dispersion strengthened iron alloys part 2 – physical interpretation of yield strength. Materials Science and Technology **14**, 1221–1226 (1998)
7. Canny, J.: A computational approach to edge detection. IEEE Transactions on Pattern Analysis and Machine Intelligence **PAMI-8**(6), 679–698 (1986)
8. Chen, C.F.R., Fan, Q., Panda, R.: Crossvit: Cross-attention multi-scale vision transformer for image classification. In: Proceedings of the IEEE/CVF international conference on computer vision. pp. 357–366 (2021)
9. Dominik, B., Johannes, W., Andreas, S., Frank, M.: Identifying and quantifying microstructures in low-alloyed steels: A correlative approach. Metallurgia Italiana pp. 5–10 (2017)
10. He, K., Zhang, X., Ren, S., Sun, J.: Deep residual learning for image recognition. In: Proceedings of the IEEE conference on computer vision and pattern recognition. pp. 770–778 (2016)
11. Jaśkowiec, K., Wilk-Kołodziejczyk, D., Bartlomiej, S., Reczek, W., Bitka, A., Małysza, M., Doroszewski, M., Pirowski, Z., Boroń, Ł.: Assessment of the quality and mechanical parameters of castings using machine learning methods. Materials **15**(8), 2884 (2022)

ICCS Camera Ready Version 2023
To cite this paper please use the final published version:
DOI: 10.1007/978-3-031-36030-5_42

12. Javier, N., Igor, S., Yoseba, P., Sendoa, R., Mikel, S., Pablo, B.: Mechanical properties prediction in high-precision foundry production. Conferences (2009)
13. Jessica, G., Dominik, B., Thorsten, S., Marc, W., Andreas, S., Marc, L., Frank, M.: Advanced microstructure classification using data mining methods. Computational Materials Science **148**, 324–335 (2018)
14. Jin, H., Chollet, F., Song, Q., Hu, X.: AutoKeras: An AutoML library for deep learning. Journal of Machine Learning Research **24**(6), 1–6 (2023)
15. John, V., Stan, D.: Improved ferrite number prediction model that accounts for cooling rate effects part 1: Model development details of a prediction model based on a neural network system of analysis are described. Welding Journal **83** (2003)
16. Liu, Z., Mao, H., Wu, C.Y., Feichtenhofer, C., Darrell, T., Xie, S.: A ConvNet for the 2020s. In: Proceedings of the IEEE/CVF Conference on Computer Vision and Pattern Recognition. pp. 11976–11986 (2022)
17. Michalski, R.S.: Attributional calculus: A logic and representation language for natural induction. Tech. Rep. MLI 04-2, George Mason University (2004)
18. Olson, D.L.: Prediction of austenitic weld metal microstructure and properties. Welding journal **64**(10), 281s–295s (1985)
19. Pajor, A., Żołnierek, J., Sniezynski, B., Sitek, A.: Effect of feature discretization on classification performance of explainable scoring-based machine learning model. In: Computational Science–ICCS 2022: 22nd International Conference, London, UK, June 21–23, 2022, Proceedings, Part III. pp. 92–105. Springer (2022)
20. Penya, Y.K., Bringas, P.G., Zabala, A.: Advanced fault prediction in high-precision foundry production. In: 2008 6th IEEE International Conference on Industrial Informatics. pp. 1672–1677 (2008). https://doi.org/10.1109/INDIN.2008.4618372
21. Rati, S., Khwaja, M.: Formation, quantification and significance of delta ferrite for 300 series stainless steel weldments. International Journal of Engineering Technology, Management and Applied Sciences **3**, 23–36 (2015)
22. Sachin, S., Andrew, B., Patrick, Trimby, G., Proust, Simon, R., Julie, C.: An automated method of quantifying ferrite microstructures using electron backscatter diffraction (ebsd) data. Ultramicroscopy **137**, 40–47 (2013)
23. Sandler, M., Howard, A., Zhu, M., Zhmoginov, A., Chen, L.C.: Mobilenetv2: Inverted residuals and linear bottlenecks. In: Proceedings of the IEEE conference on computer vision and pattern recognition. pp. 4510–4520 (2018)
24. Simonyan, K., Zisserman, A.: Very deep convolutional networks for large-scale image recognition. arXiv preprint arXiv:1409.1556 (2014)
25. Tan, M., Le, Q.: Efficientnet: Rethinking model scaling for convolutional neural networks. In: Int. conf. on machine learning. pp. 6105–6114. PMLR (2019)
26. Tan, M., Le, Q.: Efficientnetv2: Smaller models and faster training. In: International conference on machine learning. pp. 10096–10106. PMLR (2021)
27. Tripathi, M.: Analysis of convolutional neural network based image classification techniques. Journal of Innovative Image Processing (JIIP) **3**(02), 100–117 (2021)
28. Vitek, J., David, S., Hinman, C., et al.: Improved ferrite number prediction model that accounts for cooling rate effects-part 2: Model results. Welding Journal **82**(2), 43–S (2003)
29. Wilk-Kołodziejczyk, D., et al.: Selection of casting production parameters with the use of machine learning and data supplementation methods in order to obtain products with the assumed parameters
30. Yuxuan, W., Xuebang, W., Xiangyan, L., Zhuoming, X., Rui, L., Wei, L., Yange, Z., Yichun, X., Changsong, L..: Prediction and analysis of tensile properties of austenitic stainless steel using artificial neural network. Metals 2020 (2020)

ICCS Camera Ready Version 2023
To cite this paper please use the final published version:
DOI: 10.1007/978-3-031-36030-5_42